



1 Strong temporal variation in treefall and branchfall rates in a tropical 2 forest is explained by rainfall: results from five years of monthly drone 3 data for a 50-ha plot

4

5 Raquel Fernandes Araujo¹, Samuel Grubinger², Carlos Henrique Souza Celes¹, Robinson I. Negrón-
6 Juárez³, Milton García¹, Jonathan P. Dandois⁴, and Helene C. Muller-Landau¹

7

8 ¹Center for Tropical Forest Science-Forest Global Earth Observatory, Smithsonian Tropical Research Institute, Balboa, Ancon,
9 PO Box 0843-03092, Panama

10 ²Department of Forest Resources Management, University of British Columbia, 2424 Main Mall, Vancouver, BC V6T 1Z4,
11 Canada

12 ³Climate Sciences Department, Lawrence Berkeley National Laboratory, 1 Cyclotron Road, Berkeley, CA 94720, USA

13 ⁴Johns Hopkins University, Facilities and Real Estate, 3910 Keswick Rd. Suite N3100 Baltimore, MD 21211, USA

14

15 *Correspondence to:* Raquel Fernandes Araujo (araujo.raquelf@gmail.com)

16

17 **Abstract.** A mechanistic understanding of how tropical tree mortality responds to climate variation is urgently needed to predict
18 how tropical forest carbon pools will respond to anthropogenic global change, which is altering the frequency and intensity of
19 storms, droughts, and other climate extremes in tropical forests. We used five years of approximately monthly drone-acquired
20 RGB imagery for 50 ha of mature tropical forest on Barro Colorado Island, Panama, to quantify spatial structure, temporal
21 variation, and climate correlates of canopy disturbances, i.e., sudden and major drops in canopy height due to treefalls, branchfalls,
22 or collapse of standing dead trees. Treefalls accounted for 77 % of the total area and 60 % of the total number of canopy
23 disturbances in treefalls and branchfalls combined. The size distribution of canopy disturbances was close to a power function for
24 sizes above 25 m², and best fit by a Weibull function overall. Canopy disturbance rates varied strongly over time and were higher
25 in the wet season, even though windspeeds were lower in the wet season. The strongest correlate of temporal variation in canopy
26 disturbance rates was the frequency of 1-hour rainfall events above the 99.4th percentile (here 35.7 mm hour⁻¹, $r = 0.67$). We
27 hypothesize that extreme high rainfall is associated with both saturated soils, increasing risk of uprooting, and with gusts having
28 high horizontal and vertical windspeeds that increase stresses on tree crowns. These results demonstrate the utility of repeat drone-
29 acquired data for quantifying forest canopy disturbance rates over large spatial scales at fine temporal and spatial resolution, thereby
30 enabling strong tests of linkages to drivers. Future studies should include high frequency measurements of vertical and horizontal
31 windspeeds and soil moisture to better capture proximate drivers, and incorporate additional image analyses to quantify standing
32 dead trees in addition to treefalls.

33

34 1 Introduction

35 Tropical forests account for two-thirds of terrestrial biomass carbon stocks (Pan et al., 2013), and uncertainty regarding
36 the future of these stocks is a major contributor to uncertainty in the future global carbon cycle (Cavaleri et al., 2015). Tropical



37 forest carbon stocks depend critically on tree mortality rates, and theory and evidence suggest tropical tree mortality rates may be
38 increasing due to anthropogenic global change (Brienen et al., 2015; McDowell et al., 2018). Tropical tree mortality can be caused
39 by a diversity of drivers including storms, droughts, fires, lightning strikes, and biotic agents (McDowell et al., 2018; Yanoviak et
40 al., 2017; Fontes et al., 2018; Silva et al., 2018). The frequency of extreme rainfall and drought events is expected to increase in
41 tropical regions, potentially increasing associated tree mortality (IPCC, 2014; Deb et al., 2018; Aubry-Kientz et al., 2019). An
42 improved understanding of the processes of forest disturbance is critical to constrain estimates of current and future carbon cycling
43 in tropical forests under alternative emissions scenarios (Leitold et al., 2018).

44 Despite the importance of tree mortality to forest structure and carbon turnover rates, the mechanisms underlying tree
45 mortality remain unclear (McDowell et al., 2018). A key problem is that remeasurement intervals of permanent plots average five
46 or more years, making it difficult to link mortality variation with particular climatic events (Phillips et al., 2010; Davies et al.,
47 2021; Arellano et al., 2019). The high rates of decomposition in tropical forests further obscure evidence of underlying mechanisms
48 and risk factors (Arellano et al., 2019). The few studies that have quantified temporal variation of tree mortality at monthly and bi-
49 monthly scales using ground-based data have all found higher tree mortality in times of higher rainfall (Brokaw, 1982; Fontes et
50 al., 2018; Aleixo et al., 2019). This is consistent with the understanding that many trees die in treefalls, which are proximately
51 caused by trunk breakage or uprooting, and are associated with storms (Marra et al., 2014; Araujo et al., 2017; Fontes et al., 2018;
52 Negrón-Juárez et al., 2018; Esquivel-Muelbert et al., 2020). The collection of additional high temporal resolution mortality data
53 over large areas, together with high temporal resolution climatological data, can aid in linking mortality to particular climatic
54 events and thereby elucidating mortality mechanisms (Arellano et al., 2019; McMahon et al., 2019).

55 Drone-acquired aerial imagery and photogrammetry software now provide excellent tools for monitoring forest canopies
56 (Araujo et al., 2020) and repeat drone flights can quantify canopy dynamics over large areas at high temporal resolution.
57 Photogrammetric analysis of simple RGB imagery enables reconstruction of the appearance and three-dimensional structure of the
58 top of the canopy at high spatial resolution (Dandois and Ellis, 2013; Araujo et al., 2020; Zahawi et al., 2015). Comparison of
59 photogrammetry products from successive drone flights allows easy detection and quantification of treefalls and branchfalls of
60 canopy trees. Canopy trees constitute a high proportion of stem density, aboveground carbon stocks and wood productivity (Araujo
61 et al., 2020), and thus information on their dynamics is disproportionately useful. Treefalls do not necessarily result in tree
62 mortality (trees may survive and resprout), but all treefalls and branchfalls result in a large flux of carbon (wood) from biomass to
63 necromass, i.e., biomass turnover, which translates to reduced woody residence time. Periods of higher canopy disturbance rates
64 thus represent periods of higher biomass turnover, and likely correlate with higher tree mortality rates. Further, even when trees
65 don't die from a canopy disturbance event, suffering crown loss or damage increases the risk of subsequent mortality (Arellano et
66 al., 2019).

67 Monitoring canopy disturbances with drones also provides the opportunity to precisely quantify the size distributions of
68 these canopy disturbances, and to distinguish branchfalls from treefalls. Here we define a canopy disturbance as a substantial
69 decrease in canopy height in a contiguous patch of canopy occurring over one measurement interval, such as typically results from
70 a treefall or branchfall. Marvin and Asner (2016) and Dalagnol et al. (2021) referred to these as “dynamic canopy gaps.” By
71 definition, canopy disturbances reduce canopy height and thereby change light regimes for understory and neighboring trees, and
72 the magnitude of the change depends on the disturbance size in area and depth (Hubbell et al., 1999). In general, larger canopy
73 disturbances cause larger canopy gaps as traditionally measured on the ground. Previous studies have analyzed the size distributions
74 of static gaps for insights into forest structure, habitat niches, and disturbance regimes (e.g., Manrubia and Solé, 1997; Lobo and
75 Dalling, 2013, 2014; Fisher et al., 2008). Tree species respond differently to canopy gaps of different sizes, with small gaps favoring



76 a different set of species than large gaps (Brokaw, 1985; Denslow, 1980, 1987; Dalling et al., 2004). Branchfalls, like treefalls, are
77 important in generating canopy gaps and contributing to woody turnover, but also often go unmeasured (Marvin and Asner, 2016;
78 Leitold et al., 2018). Quantifying tree mortality and other non-fatal damage such as branchfall thus contributes to a better
79 understanding on change of forest structure, necromass estimates and nutrient cycling.

80 Here, we use 5 years of ~monthly drone-acquired RGB imagery for a 50 ha area of mature tropical forest on Barro
81 Colorado Island, Panama, to investigate canopy dynamics at high temporal resolution. We aim to (1) quantify temporal variation
82 in canopy disturbance rates and its relationship to climate variation; (2) characterize the size structure of canopy disturbances; and
83 (3) evaluate the role of branchfalls in canopy dynamics. We expect that disturbance rates will be higher in the wet season than the
84 dry season, and will increase with the frequency of extreme rainfall and wind events, and we compare models differing in the
85 conditions for defining such extreme events. To characterize the size structure of canopy disturbances, we quantify the size (area)
86 distribution and evaluate whether it is best fit by power, Weibull, or exponential functions. Finally, we quantify the proportion of
87 canopy disturbance due to branchfalls (rather than treefalls), and test whether branchfalls and treefalls exhibit similar patterns of
88 temporal variation. Our results provide new insights into the patterns and drivers of canopy disturbance and tree mortality in this
89 tropical forest, and illustrate the utility of drones for quantifying canopy dynamics over large areas at high temporal resolution.

90

91 **2. Methods**

92

93 **2.1 Study site**

94 Barro Colorado Island (BCI; 9°9' N, 79°50' W) is a 15 km² island in Central Panama, that was isolated from surrounding
95 mainland when Lake Gatun was created as part of the construction of the Panama Canal. BCI supports tropical moist forest in the
96 Holdridge Life Zone System (Holdridge, 1947). Annual precipitation averages approximately 2600 mm, with a pronounced dry
97 season between January and April (a mean of about 3.5 months with < 100 mm mo⁻¹). Mean annual temperature is 26 °C and varies
98 little throughout the year (Windsor, 1990). The 50 ha forest dynamics plot (1000 m x 500 m) was established on BCI in 1981
99 (Hubbell et al., 1999). It is located in old-growth forest (Leigh, 1999), with the exception of a small area of 1.92 ha of old secondary
100 forest (~100 years old) in the north central part of the plot (Harms et al., 2001).

101

102 **2.2 Meteorological data**

103 Meteorological data were collected in the lab clearing and Lutz tower, approximately 1.7 km NE of the center of the 50
104 ha plot. Wind speed was measured using an anemometer (RM Young Wind Monitor Model 05103) installed at the top of Lutz
105 tower, at 48 m height above ground and approximately 6 m above the top of the surrounding canopy. The maximum wind speed
106 was recorded for every 15 minute-interval. Rainfall was measured in the lab clearing using a tipping bucket (Hydrological Services
107 Model TB3), and recorded every 5 minutes; we aggregated these data to 15-minute periods to match the temporal resolution of the
108 wind speed data. Rainfall and wind speed data are available in
109 https://biogeodb.stri.si.edu/physical_monitoring/research/barrocolorado. The meteorological record had no gaps during our study
110 period (Fig. S1).



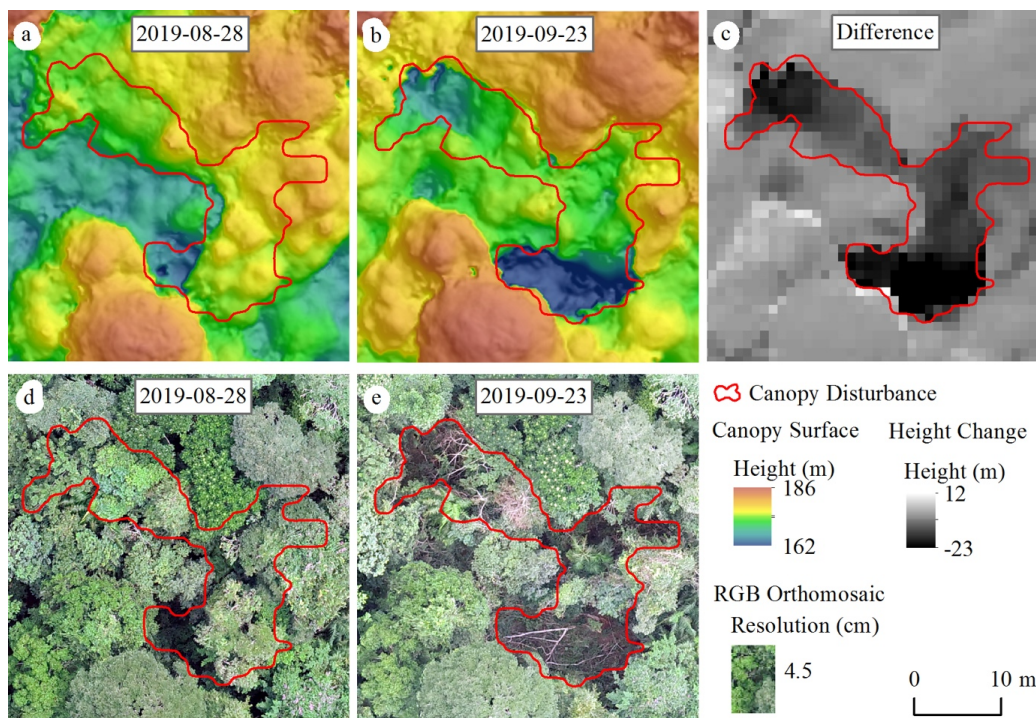
111

112 **2.3 Canopy disturbance identification**

113 We used approximately monthly orthomosaics and canopy surface models produced from drone-acquired imagery to
114 analyze temporal variation in canopy disturbance rates in the 50 ha plot between 2 October 2014 and 28 November 2019. RGB
115 imagery was collected using a variety of drones and cameras over the years, with a horizontal spatial resolution of 3-7 cm. Imagery
116 for each sampling date was processed using the photogrammetry software Agisoft Metashape to obtain orthomosaics and surface
117 elevation models, which were then aligned vertically and horizontally (details in Text S1).

118 We defined a canopy disturbance as a substantial decrease in canopy height in a contiguous patch of canopy occurring
119 over one measurement interval, such as typically results from a treefall or branchfall. We identified canopy disturbances through
120 a combination of analysis of the canopy surface model changes and visual interpretation of the orthomosaics (Fig. 1). We first
121 differenced surface elevation models for successive dates to obtain a raster of the canopy height changes for the associated interval
122 (Fig. 1, Text S1). We then pre-delineated major canopy disturbances by filtering for areas in which canopy height decreased more
123 than 10 m in contiguous areas of at least 25 m² (the minimum area for canopy gaps in previous studies by Brokaw (1982) and
124 Hubbell et al. (1999)), and that had an area-to-perimeter ratio greater than 0.6. (The area-to-perimeter condition removes artifacts
125 associated with slight shifts in the measured positions of individual trees from one image set to another, whether due to wind or
126 alignment errors.) Finally, we systematically examined orthomosaic images for 1-ha square subplots for each pair of successive
127 dates and edited the pre-delineated polygons, removed false positives, and added visible new canopy disturbances that were not
128 previously delineated (whether because they were too small in area or in canopy height drop). During the visual inspection of the
129 data for the last three years we also classified disturbances as being due to treefalls (a whole previously live tree fell, creating a
130 clearly visible gap on the forest floor, or the whole live crown disappeared), branchfalls (a portion of a live crown broke), or
131 standing dead trees disintegrating (Fig. S2).

132



133

134 **Figure 1.** Canopy disturbance visualized on canopy surface models and orthomosaics calculated from photogrammetric analyses
135 of drone imagery. (a,b) Elevation models for a portion of the study area on two successive dates, 28 August 2019 (a) and 23
136 September 2019 (b). (c) Difference in elevation between the two dates, with black area indicating large decrease in canopy
137 elevation. (d,e) RGB orthomosaics of the same dates.

138 We calculated the total number and area of canopy disturbances within the BCI 50 ha plot during the five years of the
139 study. In calculating the number and total area of disturbances, we included all disturbed areas that were inside the plot boundaries
140 (if a disturbance was on the boundary, only the area inside the plot was included). Our analyses of temporal variation employed
141 the same definitions for numbers and areas of canopy disturbances within the 50 ha plot. For analyses of the size structure of
142 disturbances, we included the complete areas of disturbances whose centroids were located within the plot (i.e., we excluded
143 disturbances centered outside the plot, and included area outside the plot for disturbances centered inside the plot to avoid artifacts
144 related to reducing disturbance size by trimming at the plot boundaries).

145

146 2.4 Temporal variation in canopy disturbance rates and its relation to climate

147 We calculated canopy disturbance rates for each measurement interval as the percentage of area disturbed per month
148 (i.e., per 30-day period). Specifically, we summed the total area disturbed during the measurement interval, and divided by the
149 total area of the plot and the length of the time interval. We excluded one excessively long interval (237 days) from all analyses of
150 temporal variation; the remaining intervals ranged from 14 to 91 days, with a median of 31.5 days (Table S1). We also calculated
151 an incidence canopy disturbance rate as the *number* of canopy disturbances per hectare per month. We calculated the mean,



152 minimum, maximum, and the 25th, 50th, and 75th percentiles of interval length in days, number and area of canopy disturbances,
153 and the respective monthly rates.

154 We compared canopy disturbance rates between wet and dry seasons and between early wet and late wet seasons. We
155 defined the dry season as January 1 to April 30 (rainfall < 100 mm mo⁻¹, Fig. S3), the early wet season as 1 May to 31 August, and
156 the late wet season as 1 September to 31 December. Intervals that straddled more than one season were classified to the season in
157 which they had more days. We tested for homogeneity of variances using the Levene test, and for differences between means using
158 the two-tailed Student's t-test for the log-transformed canopy disturbance rates.

159 We evaluated the relationship of temporal variation in canopy disturbance rates with temporal variation in climate
160 extremes using linear regressions. We regressed canopy disturbance rates (area per time) against the frequency of extreme rainfall
161 and windspeed events (number per time), for different definitions of extreme events. For example, one definition of an extreme
162 event would be a 15-minute period with rainfall above the 99th percentile. We evaluated three different temporal grains for defining
163 extreme events (15-minute, 1-hour, and 1-day intervals), for two different meteorological variables (total rainfall and maximum
164 windspeed), and 100 different thresholds, corresponding to every 0.1 percentile increment between the 90th and 99.9th percentile
165 of the corresponding distributions. We compared the predictive ability of these 600 different definitions of extreme events in terms
166 of their Pearson correlations.

167

168 2.5 Size structure of canopy disturbances

169 We characterized the size structure of canopy disturbances whose geometric center was inside the plot, excluding
170 disturbances from the one excessively long interval of 237 days. (Longer time intervals increase the likelihood that what is
171 measured as a single disturbance event in fact constitutes multiple adjoining or overlapping events.) We calculated the mean,
172 minimum, maximum, and median of area of individual canopy disturbances. We graphed the cumulative distribution functions
173 with respect to individual disturbance area of number and area of canopy disturbances, to quantify the proportions of canopy
174 disturbances and of total area disturbed below any given size.

175 We took advantage of the three-dimensional structure of our photogrammetry data to quantify canopy disturbances in
176 terms of their vertical height drop as well as their horizontal area. For each canopy disturbance, we calculated the average height
177 drop from the differences in the canopy surface models. (We excluded 61 canopy disturbances in which heights increased because
178 they reflect errors in the canopy height models.) We evaluated how average height drop was related to area across canopy
179 disturbances, graphically and in terms of their Pearson correlation.

180 We quantified the size distributions of canopy disturbances by fitting three alternative probability distributions:
181 exponential, power, and Weibull. Recognizing that our methods may miss smaller disturbances, we fit these distributions to
182 truncated datasets, excluding disturbances below 2, 5, 10 or 25 m². (Note that 25 m² is the minimum area for defining a canopy
183 disturbance in our automated pre-delineation algorithm, and we are confident we captured all disturbances above this area.) We
184 binned the data into 1 m² classes, and fitted each distribution to each truncated dataset using maximum likelihood, as described in
185 (Araujo et al., 2020). We compared the goodness of fit of the different functions using Akaike's Information Criterion (AIC).



186

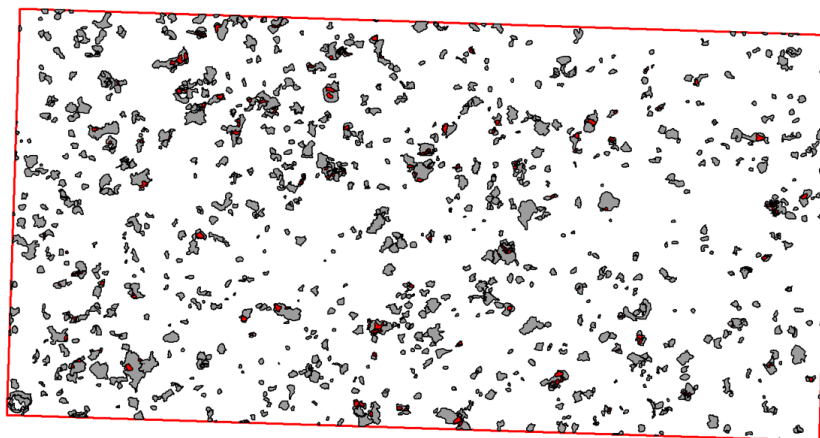
187 2.6 Branchfalls vs. treefalls

188 For the last three years, for which we classified each canopy disturbance as being a branchfall, treefall, or standing dead
189 tree, we evaluated the relative contributions of branchfalls vs. treefalls. We did not include standing dead trees in the analysis
190 because our methods possibly missed many standing dead trees. We separately calculated treefall and branchfall disturbance rates
191 for each interval, and relative contributions to their summed number and area. We regressed branchfall disturbance rates against
192 treefall disturbance rates, for both area- and number-based rates, and calculated their Pearson correlations.

193

194 3. Results

195 We identified 1056 canopy disturbances with a combined area of 56,595.12 m² that affected the area within the BCI 50
196 ha plot between 2 October 2014 and 28 November 2019 (Fig. 2). During the 5 years of the study, 10.7 % of the area of the BCI
197 50-ha plot was affected by canopy disturbances, and 0.7 % was disturbed more than once (Fig. 2).



198

199 **Figure 2.** Map of canopy disturbances on the 50 ha plot (red rectangle, 1000 x 500 m) on Barro Colorado Island, Panama, from 2
200 October 2014 to 28 November 2019. Areas that were disturbed a single time are shown in grey, those disturbed more than once
201 in red.

202

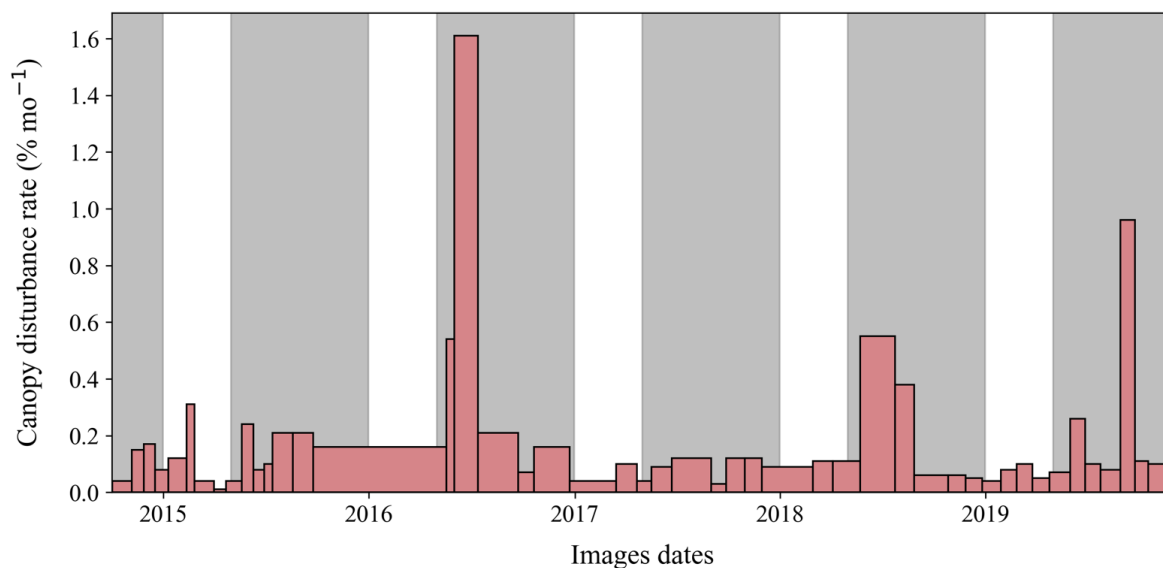
203 3.1 Temporal variation in canopy disturbance rates

204 Temporal variation analyses included 906 disturbances or partial disturbances encompassing 50,202.8 m² of area that
205 were located inside the 50 ha plot and were not part of the excluded long interval. There was strong temporal variation in canopy
206 disturbance rates among the 46 time intervals analyzed, with parallel variation in the total area disturbed (Fig. 3) and the number
207 of disturbances (Fig. S4). The mean rate of canopy disturbance creation was 916 m² mo⁻¹ (range of 75 m² mo⁻¹ to 8040.9 m² mo⁻¹)



208 and median $499 \text{ m}^2 \text{ mo}^{-1}$ (other statistics in Table S1).

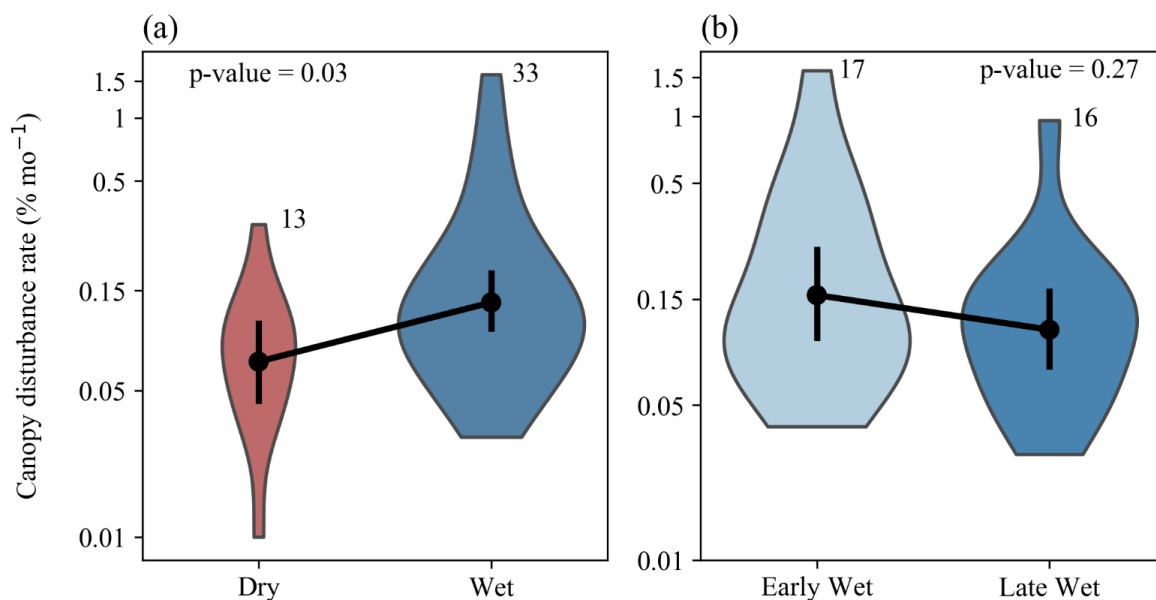
209 The highest disturbance rates occurred during May-July 2016, May-August 2018, and August-September 2019 (Fig. S5).
210 The single highest disturbance rate was observed between 1 June and 13 July 2016, when $11,257 \text{ m}^2$ of disturbances were created
211 in just 42 days (a rate of $268 \text{ m}^2 \text{ day}^{-1}$). A full 2.3 % of the total area of the plot was converted to new canopy disturbances during
212 this time interval. In contrast, the total area of new disturbances across the rest of the 5-year period was $38,946 \text{ m}^2$ (a rate of 24.3
213 $\text{m}^2 \text{ day}^{-1}$).



214

215 **Figure 3.** Temporal variation in canopy disturbance rates in the 50 ha plot on Barro Colorado Island, Panama, across measurement
216 intervals. Gray shading indicates the wet seasons (May to December) of each year and ticks on the x axis indicate the first day of
217 each year. Rates are shown in units of percent of area per month (30-day period). Note that the total area of each rectangle is
218 proportional to the total area of canopy disturbed during that measurement interval.

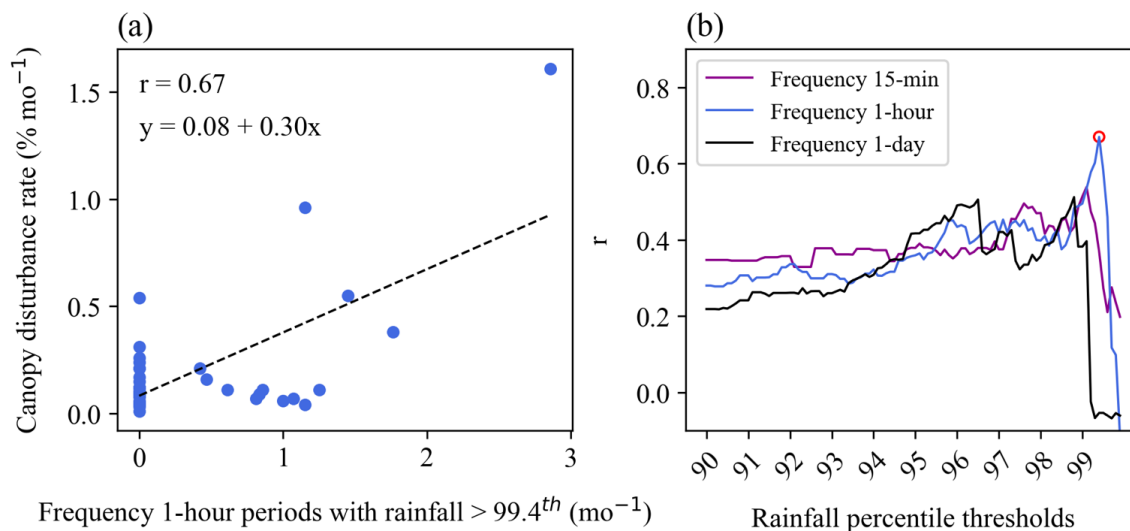
219 Rates of canopy disturbances were higher during the wet season ($p = 0.03$; Fig. 4a). There was no significant difference
220 in rates between the early and late wet season ($p = 0.27$, Fig. 4b). Very high rates of disturbance ($> 0.3 \%$ per month) were observed
221 only in the wet season.



222

223 **Figure 4.** Comparisons of canopy disturbances rates between wet and dry seasons (a), and between early and late wet seasons (b).
224 Violin plots depict the distributions of disturbance rates (% area disturbed per month) over time intervals, with the number of time
225 intervals listed above each violin plot. Black dots and bars show means and 95% confidence intervals, respectively.

226 The best predictor of temporal variation in canopy disturbance rates was the frequency of 1-hour rainfall events above the
227 99.4th percentile, here 35.7 mm hour⁻¹, which explained 45 % of the variation (Fig. 5a). This threshold outperformed all other tested
228 rainfall thresholds (all percentiles from 90.0 to 99.9, by 0.1 % of the different frequency time scales – Fig. 5b). Only two of these
229 high rainfall events occurred during the same day (Table S2). The measurement interval with the highest disturbance rate (June 1
230 to July 13 2016) included four such high rainfall events: 41.7 mm hour⁻¹ on June 17, 41.9 mm hour⁻¹ on June 23, 49.3 mm hour⁻¹
231 on June 30, and 36.1 mm hour⁻¹ on July 4 (Table S2). The frequency of high horizontal maximum wind speed events was not
232 significantly related with canopy disturbance rates. Indeed, Pearson correlations were negative for almost all wind speed variables
233 (Fig. S6).



234

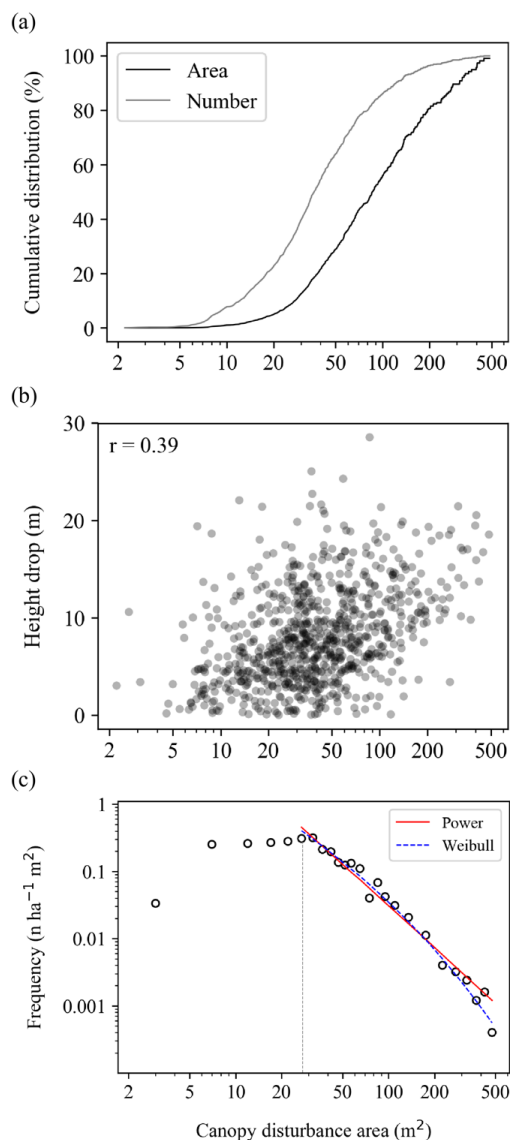
235 **Figure 5.** Relation of temporal variation in canopy disturbance rates to the frequency of extreme rainfall events. (a) The relationship
236 for the single best predictor of canopy disturbance rate: the frequency of 1-hour periods with rainfall exceeding the 99.4th percentile;
237 each point represents one measurement interval, and the dashed line shows the linear regression. (b) Variation in Pearson
238 correlation between canopy disturbance rate and frequency of extreme rainfall events depending on the temporal grain (colors) and
239 percentile threshold (x axis) for defining extreme rainfall events; the open red circle indicates the best correlation.

240

241 3.2 Size structure of canopy disturbances

242 A total of 878 canopy disturbances with 49,958 m² total area had their centers inside the plot and were not part of the
243 excluded long interval, and thus were included in the size distribution analyses. The areas of mapped individual canopy
244 disturbances ranged from 2.2 m² to 486.7 m², with a mean of 56.9 m². The median disturbance area was 36.4 m², whereas 50 % of
245 the total area was in disturbances greater than 86.6 m² (see Fig. 6a for the full cumulative distributions by gap number and area).
246 Canopy disturbances with larger areas tended to have larger mean decreases in canopy height (Pearson $r = 0.39$, Fig. 6b).

247 The size distribution of canopy disturbances was close to a power function for areas above 25 m², and was relatively flat
248 over the range of 5 to 25 m² (Fig. 6c). The fitted exponent of the power function was -1.96 for canopy disturbances above 25 m²,
249 but the Weibull distribution provided a better fit than the power function (Table 1). When distributions were fit to data including
250 smaller size classes (> 2 m², > 5 m² or > 10 m²), the distribution is further from a power function; the Weibull remains the best fit,
251 the exponential becomes the second-best fit, and the power function the worst fit of the three (Fig. S7, Table S3).



252

253 **Figure 6.** Size structure of canopy disturbances. (a) Cumulative number and area of canopy disturbances in relation to their area.
254 (b) Relationship of mean vertical height drop to horizontal area among canopy disturbances. (c) Size distribution of canopy
255 disturbances, together with Weibull and power function fits for canopy disturbances larger than 25 m² (this threshold was chosen
256 because we are confident we identified all canopy disturbances above this area, but we may have missed some smaller ones). The
257 vertical dashed gray line indicates the 25 m² threshold.

258

259



260 **Table 1.** Parameter values and delta AIC values for maximum likelihood fits of exponential, power and Weibull probability density
261 functions to size distributions for canopy disturbances larger than 25 m². Delta AIC is the difference in AIC from the best model.
262 The best-fit model is highlighted in bold.

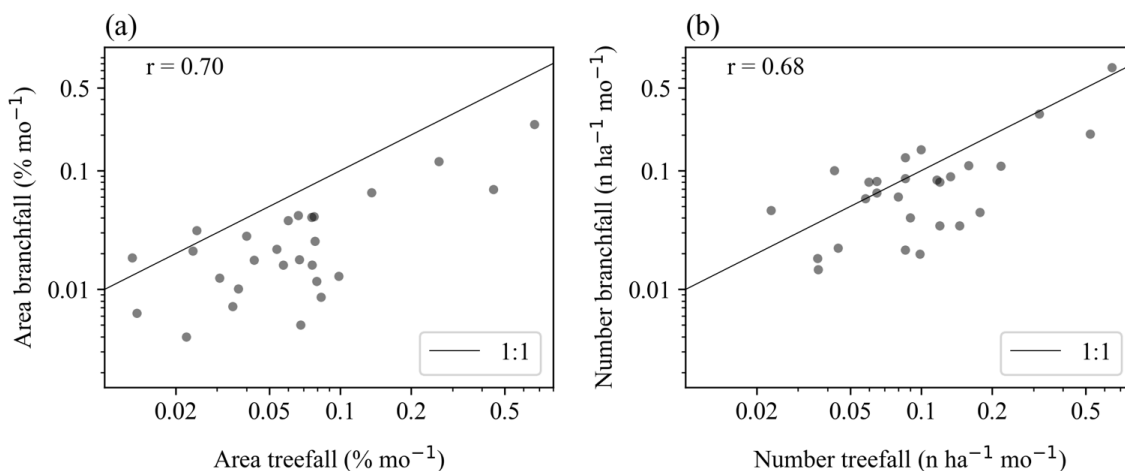
Distribution	λ	k	Delta AIC
Exponential	0.020		62.45
Power	1.963		16.50
Weibull	6.745	0.448	0.00

263

264

265 3.3 Treefalls and branchfalls

266 A total of 411 canopy disturbances with 23,289.9 m² total area occurred during the final three years, and thus were
267 included in the analyses of branchfall contributions. Branchfalls accounted for 23 % of the total area and 40 % of total number of
268 disturbances in treefalls and branchfalls combined. Treefall and branchfall disturbance rates varied largely in parallel (Fig. 7, Fig.
269 S8). Branchfalls were a larger proportion of events and area in some measurement periods than others. The ratio of area in
270 branchfalls to area in treefalls ranged from 0.07 to 1.4 among measurement periods (Fig. 7a), and the ratio of number of branchfalls
271 to number of treefalls ranged from 0.2 to 2.3 (Fig. 7b). Standing dead trees accounted for 6.6 % of the total number and 6.7 % of
272 the total area of mapped canopy disturbances.



273

274 **Figure 7.** Relationship of temporal variation in branchfall rates to temporal variation in treefall rates, when measured by total area
275 (a) and number of events (b). This includes measurement intervals from 23 December 2016 to 28 November 2019.

276



277 4. Discussion

278 The use of high frequency (approximately monthly) drone imagery enabled us to quantify temporal variation in canopy
279 disturbance rates and to quantify the sizes of canopy disturbances at high temporal and spatial resolutions. We found that canopy
280 disturbance rates of the BCI 50 ha plot varied strongly over time, and were higher in the wet season. The frequency of extreme
281 rainfall events was the single best predictor of monthly variation in canopy disturbance rate during the 5-year study period. In
282 contrast, maximum horizontal wind speed was not significantly related. The size distribution of canopy disturbances was close to
283 a power function for larger canopy disturbances, but best fit by a Weibull function overall. Branchfalls accounted for 23 % of the
284 total area of disturbances from treefalls and branchfalls combined, and branchfall rates varied largely in parallel with treefall rates
285 over time. These findings contributed to an improved understanding of the size distribution, temporal variation and meteorological
286 drivers of canopy disturbances in tropical forests.

287 4.1 Temporal variation in canopy disturbance

288 Canopy disturbance rates varied strongly over time in this moist tropical forest, and were higher in the wet season. A
289 single time interval (June 1 to July 13 2016) accounted for 21 % of the total disturbed area of the BCI 50-ha plot. Treefall and
290 branchfall disturbance rates varied largely in parallel, but not entirely. Some of the differences in temporal patterns simply reflect
291 the stochastic nature of these processes, but different temporal patterns in branchfalls vs. treefalls could also reflect different
292 sensitivity to particular abiotic drivers (e.g. wind regime, soil saturation). The frequency of rainfall events $> 35.7 \text{ mm hour}^{-1}$
293 explained much of the variation in canopy disturbance rates among measurement intervals, whereas the frequency of high
294 maximum horizontal wind speeds was not related. At our site, horizontal wind speeds are higher during the dry season, when
295 canopy disturbance rates are lower (Fig. 4a, Fig. S1). We hypothesize that extreme high rainfall is associated with both saturated
296 soils, increasing risk of uprooting, and with gusts having high horizontal and vertical windspeeds that increase stresses on tree
297 crowns. Future studies should include high frequency measurements of vertical and horizontal windspeeds and soil moisture to
298 better capture proximate drivers, and evaluate mechanistically formulated predicted models that include multiple variables.

299 These results are consistent with previous findings on seasonal variation and the role of rainfall in gap formation in tropical
300 forests. A previous 4-year study on BCI found seasonal peaks in August and September, in the middle of the wet season, with
301 monthly treefall rates significantly correlated with rainfall ($r = 0.47$, $p < 0.02$) (Brokaw, 1982). Tree mortality was also strongly
302 and positively correlated with monthly rainfall ($r = 0.85$) in a 1-year study of a 10-ha site in the Central Amazon (Fontes et al.,
303 2018). A study monitored canopy trees monthly over five decades in the Central Amazon and found that trees died more often
304 during wet months, even in drought years (Aleixo et al., 2019). A regional study of the Central Amazon based on 12 years of
305 satellite data found that major windthrows (visible on LANDSAT) occurred more frequently between September and February,
306 months characterized by heavy rainfall, than the rest of the year (Negrón-Juárez et al., 2017). Analysis of spatial variation in forest
307 damage from Hurricane María in Puerto Rico found that total rainfall was the most important meteorological risk factor and
308 maximum sustained one-minute wind speeds the second-most-important; these two variables were moderately correlated ($r = 0.43$)
309 (Hall et al., 2020).

310 Multiple studies have highlighted the importance of mesoscale convective systems, such as squall lines, for windthrows
311 (Garstang et al., 1998; Negrón-Juárez et al., 2010, 2017; Araujo et al., 2017). In Panama, the period of June to August has the
312 higher number of mesoscale convective systems (Jaramillo et al., 2017), and these were the months when we observed the highest



313 canopy disturbance rates. The threshold rainfall rate of $35.7 \text{ mm hour}^{-1}$, which defined the extreme rainfall rate that was the best
314 predictor of canopy disturbance formation in our study, is six times higher than the mean rate for mesoscale convective systems in
315 the Panama region (Jaramillo et al., 2017), highlighting the importance of extreme events.

316

317 **4.2 Mechanisms and size structure canopy disturbances**

318 Gaps in the forest canopy can be caused proximally by treefalls of canopy trees, branchfalls of canopy branches, standing
319 dead canopy trees, or senescing major canopy branches. Treefalls and branchfalls of canopy trees are well-captured in our analyses,
320 which focus on short-term changes that indicate loss of major canopy elements. In contrast, standing dead trees and senescing
321 branches generally involve more subtle changes in the canopy over a longer period of time, and may be missed by our methods.
322 Treefalls account for a majority of canopy tree mortality in most tropical forests, but standing tree mortality also plays a major
323 role, especially in drought periods. Overall, treefalls (in which trees were uprooted or their trunks snapped) accounted for 51.2 %
324 of all mortality of trees $> 10 \text{ cm DBH}$ in a large-scale study of tree mortality in 189 Amazonian plots (Esquivel-Muelbert et al.,
325 2020) and 65 % in a study that monitored tree mortality in 10 ha of forest in the Central Amazon bi-monthly over one year (Fontes
326 et al., 2018). Treefalls can involve a single canopy tree, or multiple canopy trees. Multi-tree treefalls can result from coordinated
327 disturbances over a large area (e.g., large footprint wind disturbance) and/or from domino effects in which the failure of one canopy
328 tree directly stresses one or more neighboring trees and causes them to fall as well (e.g., when additional trees are knocked down
329 by the first tree, or pulled down because of connections via lianas). It has been hypothesized that canopy disturbances may also be
330 contagious over longer time intervals, with increased risk of treefall near canopy gaps, but evidence for this in tropical forests is
331 mixed (Jansen et al., 2008). Given that our measurement intervals are relatively short (~one month), almost all of our mapped
332 canopy disturbances are likely to reflect single catastrophic events.

333 Our study is one of several that have documented size distributions of canopy disturbances (dynamic gaps) or of static
334 canopy gaps above some size that are approximately power functions, both on BCI (Solé and Manrubia, 1995; Lobo and Dalling,
335 2014) and in other tropical forests (Marvin and Asner, 2016; Asner et al., 2013; Kellner and Asner, 2009; Silva et al., 2019; Fisher
336 et al., 2008). Static canopy gaps are areas in which the forest canopy is below a threshold height, e.g., 10 m, at a given time. A
337 power function distribution of disturbance event sizes (here canopy disturbances) and of the sizes of disturbed areas (canopy gaps)
338 can emerge from self-organization of dynamic systems such as forests (Solé and Manrubia, 1995). These same self-organized
339 dynamics lead to the development of equilibrium size distributions of trees, which are typically well-fit by Weibull distributions
340 in tropical forests (Muller-Landau et al., 2006b, a). The relative dearth of canopy disturbances smaller than 25 m^2 in our dataset,
341 compared to what would be expected under a power function, may be explained in part by lower detection frequencies. Our
342 methods are expected to capture all treefall and branchfalls above this threshold, but we may increasingly have missed smaller
343 events, especially below $\sim 5 \text{ m}^2$. However, we consider it unlikely that this is a sufficient explanation for the shortfall in small
344 trees, and suggest that it is more likely explained largely by the low frequency of small trees and branches in the canopy of this
345 mature tropical forest, and thus a scarcity of small treefall and branchfall events.

346 Although rarely quantified, branchfall is an important ecological process, with major contributions to woody turnover and
347 necromass production. We found that branchfalls were almost as common as treefalls in number, although they contributed a
348 substantially smaller total area of disturbance. Similarly, a ground survey of 78 canopy turnover events in a Brazilian Amazon



349 forest found that 44 % were branchfalls, and that they accounted for 15 % of the total affected area (Leitold et al., 2018). In contrast,
350 a landscape level analysis of LiDAR data concluded that branchfalls were seven times more frequent than treefalls and accounted
351 for five times more area (Marvin and Asner, 2016). However, this study classified branchfalls and treefalls based purely on the
352 proportional decrease in canopy height (10-40 % decrease and 70-100 % decrease, respectively), a process liable to
353 misclassification, it entirely ignored disturbances involving intermediate decreases in canopy height (40-70 %), and did not
354 consider the possibility that any of these disturbances might be standing dead trees. Thus the contrast between our findings and
355 those of Marvin and Asner (2016) on the contributions of branchfalls may be due as much to methodological differences as to real
356 variation in canopy dynamics.

357

358 **5. Conclusions and future directions**

359 A mechanistic understanding of the controls on woody residence time in tropical forests is urgently needed to predict the
360 future of tropical forest carbon stocks and biodiversity under global change. Canopy trees account for a majority of the productivity
361 and carbon stocks in tropical forests, and their fates are disproportionately important for determining stand-level woody residence
362 time. Advances in drone hardware and photogrammetric software now make it relatively inexpensive and straightforward to
363 quantify forest canopy structure and dynamics at high spatial and temporal resolution through digital aerial photogrammetry and
364 repeat drone imagery acquisitions. Here we applied these methods to 50 ha of old-growth tropical forest for five years, and
365 analyzed the resulting products to quantify major drops in canopy height such as those created by branchfalls and treefalls, and
366 thus calculate the canopy disturbance rate. We found that canopy disturbance rates are highly temporally variable, and are well-
367 predicted by extreme rainfall events. Even higher temporal resolution canopy dynamics data together with higher frequency three-
368 dimensional wind data would enable an even stronger assessment of the link to storm conditions, and additional analyses of the
369 photogrammetry data could shed light on standing tree mortality. The expansion of these methods to additional and larger areas,
370 potentially in part through citizen science initiatives, has great potential to improve our understanding of tropical forest tree
371 mortality, and the future of tropical forests under changing climate regimes.

372

373 *Code and data availability.* Analysis codes, input data and output results are available at
374 https://github.com/forestgeo/gap_dynamics_BCI50ha. All files will be published in a permanent form at Smithsonian Figshare
375 repository 10.25573/data.c.5389043 when the manuscript is published in final form.

376

377 *Author contributions.* HCM and RFA planned and designed the research. MG and JD collected drone data. RFA, SG, JD and MG
378 processed drone imagery. RFA performed the analysis with support from HCM, CHSC and RINJ. RFA and HCM wrote the
379 manuscript.

380

381 *Competing interests.* The authors declare that they have no conflicts of interest.



382

383 *Acknowledgments.* We gratefully acknowledge the financial support of the Next Generation Ecosystem Experiments-Tropics,
384 funded by the U.S. Department of Energy, Office of Science, Office of Biological and Environmental Research (RFA), the
385 Smithsonian Institution Competitive Grants Program for Science (HCM, JD), and the Smithsonian Tropical Research Institute
386 fellowship program (CHSC, RFA). We thank Milton Solano, Pablo Ramos, and Paulino Villareal for assistance in collecting and
387 processing the drone imagery, and Jeffrey Chambers, KC Cushman and Evan Gora for providing helpful comments on an earlier
388 version of this manuscript.

389

390 **References**

- 391 Aleixo, I., Norris, D., Hemerik, L., Barbosa, A., Prata, E., Costa, F., and Poorter, L.: Amazonian rainforest tree mortality driven
392 by climate and functional traits, *Nat. Clim. Chang.*, 9, 384–388, <https://doi.org/10.1038/s41558-019-0458-0>, 2019.
- 393 Araujo, R. F., Nelson, B. W., Celes, C. H. S., and Chambers, J. Q.: Regional distribution of large blowdown patches across
394 Amazonia in 2005 caused by a single convective squall line: Distribution of Amazonia Blowdown Damage, *Geophys. Res. Lett.*,
395 44, 7793–7798, <https://doi.org/10.1002/2017GL073564>, 2017.
- 396 Araujo, R. F., Chambers, J. Q., Celes, C. H. S., Muller-Landau, H. C., Santos, A. P. F. dos, Emmert, F., Ribeiro, G. H. P. M.,
397 Gimenez, B. O., Lima, A. J. N., Campos, M. A. A., and Higuchi, N.: Integrating high resolution drone imagery and forest
398 inventory to distinguish canopy and understory trees and quantify their contributions to forest structure and dynamics, *PLoS*
399 *ONE*, 15, e0243079, <https://doi.org/10.1371/journal.pone.0243079>, 2020.
- 400 Arellano, G., Medina, N. G., Tan, S., Mohamad, M., and Davies, S. J.: Crown damage and the mortality of tropical trees, *New*
401 *Phytol.*, 221, 169–179, <https://doi.org/10.1111/nph.15381>, 2019.
- 402 Asner, G. P., Kellner, J. R., Kennedy-Bowdoin, T., Knapp, D. E., Anderson, C., and Martin, R. E.: Forest Canopy Gap
403 Distributions in the Southern Peruvian Amazon, *PLoS ONE*, 8, e60875, <https://doi.org/10.1371/journal.pone.0060875>, 2013.
- 404 Aubry-Kientz, M., Rossi, V., Cornu, G., Wagner, F., and Hérault, B.: Temperature rising would slow down tropical forest
405 dynamic in the Guiana Shield, *Sci Rep*, 9, 10235, <https://doi.org/10.1038/s41598-019-46597-8>, 2019.
- 406 Brien, R. J. W., Phillips, O. L., Feldpausch, T. R., Gloor, E., Baker, T. R., Lloyd, J., Lopez-Gonzalez, G., Monteagudo-
407 Mendoza, A., Malhi, Y., Lewis, S. L., Vásquez Martínez, R., Alexiades, M., Álvarez Dávila, E., Alvarez-Loayza, P., Andrade,
408 A., Aragão, L. E. O. C., Araujo-Murakami, A., Arets, E. J. M. M., Arroyo, L., Aymard C., G. A., Bánki, O. S., Baraloto, C.,
409 Barroso, J., Bonal, D., Boot, R. G. A., Camargo, J. L. C., Castilho, C. V., Chama, V., Chao, K. J., Chave, J., Comiskey, J. A.,
410 Cornejo Valverde, F., da Costa, L., de Oliveira, E. A., Di Fiore, A., Erwin, T. L., Fauset, S., Forsthofer, M., Galbraith, D. R.,
411 Grahame, E. S., Groot, N., Hérault, B., Higuchi, N., Honorio Coronado, E. N., Keeling, H., Killeen, T. J., Laurance, W. F.,
412 Laurance, S., Licona, J., Magnussen, W. E., Marimon, B. S., Marimon-Junior, B. H., Mendoza, C., Neill, D. A., Nogueira, E. M.,
413 Núñez, P., Pallqui Camacho, N. C., Parada, A., Pardo-Molina, G., Peacock, J., Peña-Claros, M., Pickavance, G. C., Pitman, N. C.
414 A., Poorter, L., Prieto, A., Quesada, C. A., Ramírez, F., Ramírez-Angulo, H., Restrepo, Z., Roopsind, A., Rudas, A., Salomão, R.
415 P., Schwarz, M., Silva, N., Silva-Espejo, J. E., Silveira, M., Stropp, J., Talbot, J., ter Steege, H., Teran-Aguilar, J., Terborgh, J.,
416 Thomas-Caesar, R., Toledo, M., Torello-Raventos, M., Umetsu, R. K., van der Heijden, G. M. F., van der Hout, P., Guimarães
417 Vieira, I. C., Vieira, S. A., Vilanova, E., Vos, V. A., and Zagt, R. J.: Long-term decline of the Amazon carbon sink, *Nature*, 519,
418 344–348, <https://doi.org/10.1038/nature14283>, 2015.
- 419 Brokaw, N. V. L.: Treefalls: frequency, timing, and consequences., in: *The ecology of a tropical forest: seasonal rhythms and*
420 *long-term changes*, Smithsonian Institution, Washington, DC, 101–108, 1982.
- 421 Brokaw, N. V. L.: Gap-Phase Regeneration in a Tropical Forest, 66, 682–687, <https://doi.org/10.2307/1940529>, 1985.
- 422 Cavaleri, M. A., Reed, S. C., Smith, W. K., and Wood, T. E.: Urgent need for warming experiments in tropical forests, *Glob*
423 *Change Biol.*, 21, 2111–2121, <https://doi.org/10.1111/gcb.12860>, 2015.



- 424 Dalagnol, R., Wagner, F. H., Galvão, L. S., Streher, A. S., Phillips, O. L., Gloor, E., Pugh, T. A. M., Ometto, J. P. H. B., and
425 Aragão, L. E. O. C.: Large-scale variations in the dynamics of Amazon forest canopy gaps from airborne lidar data and
426 opportunities for tree mortality estimates, *Sci Rep*, 11, 1388, <https://doi.org/10.1038/s41598-020-80809-w>, 2021.
- 427 Dalling, J. W., Winter, K., and Hubbell, S. P.: Variation in growth responses of neotropical pioneers to simulated forest gaps,
428 *Funct Ecology*, 18, 725–736, <https://doi.org/10.1111/j.0269-8463.2004.00868.x>, 2004.
- 429 Dandois, J. P. and Ellis, E. C.: High spatial resolution three-dimensional mapping of vegetation spectral dynamics using
430 computer vision, *Remote Sensing of Environment*, 136, 259–276, <https://doi.org/10.1016/j.rse.2013.04.005>, 2013.
- 431 Davies, S. J., Abiem, I., Abu Salim, K., Aguilar, S., Allen, D., Alonso, A., Anderson-Teixeira, K., Andrade, A., Arellano, G.,
432 Ashton, P. S., Baker, P. J., Baker, M. E., Baltzer, J. L., Basset, Y., Bissengou, P., Bohlman, S., Bourg, N. A., Brockelman, W.
433 Y., Bunyavechewin, S., Burslem, D. F. R. P., Cao, M., Cárdenas, D., Chang, L.-W., Chang-Yang, C.-H., Chao, K.-J., Chao, W.-
434 C., Chapman, H., Chen, Y.-Y., Chisholm, R. A., Chu, C., Chuyong, G., Clay, K., Comita, L. S., Condit, R., Cordell, S.,
435 Dattaraja, H. S., de Oliveira, A. A., den Ouden, J., Detto, M., Dick, C., Du, X., Duque, Á., Ediriweera, S., Ellis, E. C., Obiang,
436 N. L. E., Esufali, S., Ewango, C. E. N., Fernando, E. S., Filip, J., Fischer, G. A., Foster, R., Giambelluca, T., Giardina, C.,
437 Gilbert, G. S., Gonzalez-Akre, E., Gunatilleke, I. A. U. N., Gunatilleke, C. V. S., Hao, Z., Hau, B. C. H., He, F., Ni, H., Howe,
438 R. W., Hubbell, S. P., Huth, A., Inman-Narahari, F., Itoh, A., Janík, D., Jansen, P. A., Jiang, M., Johnson, D. J., Jones, F. A.,
439 Kanzaki, M., Kenfack, D., Kiratiprayoon, S., Král, K., Krizel, L., Lao, S., Larson, A. J., Li, Y., Li, X., Litton, C. M., Liu, Y., Liu,
440 S., Lum, S. K. Y., Luskin, M. S., Lutz, J. A., Luu, H. T., Ma, K., Makana, J.-R., Malhi, Y., Martin, A., McCarthy, C., McMahon,
441 S. M., McShea, W. J., Memiaghe, H., Mi, X., Mitre, D., Mohamad, M., Monks, L., et al.: ForestGEO: Understanding forest
442 diversity and dynamics through a global observatory network, *Biological Conservation*, 253, 108907,
443 <https://doi.org/10.1016/j.biocon.2020.108907>, 2021.
- 444 Deb, J., Phinn, S., Butt, N., and Mcalpine, C.: Climate change impacts on tropical forests: identifying risks for tropical Asia,
445 *JTFS*, 30, 182–194, <https://doi.org/10.26525/jtfs2018.30.2.182194>, 2018.
- 446 Denslow, J. S.: Patterns of plant species diversity during succession under different disturbance regimes, *Oecologia*, 46, 18–21,
447 <https://doi.org/10.1007/BF00346960>, 1980.
- 448 Denslow, J. S.: Tropical Rainforest Gaps and Tree Species Diversity, 1, 431–451, 1987.
- 449 Esquivel-Muelbert, A., Phillips, O. L., Brien, R. J. W., Fauset, S., Sullivan, M. J. P., Baker, T. R., Chao, K.-J., Feldpausch, T.
450 R., Gloor, E., Higuchi, N., Houwing-Duistermaat, J., Lloyd, J., Liu, H., Malhi, Y., Marimon, B., Marimon Junior, B. H.,
451 Monteagudo-Mendoza, A., Poorter, L., Silveira, M., Torre, E. V., Dávila, E. A., del Aguila Pasquel, J., Almeida, E., Loayza, P.
452 A., Andrade, A., Aragão, L. E. O. C., Araujo-Murakami, A., Arets, E., Arroyo, L., Aymard C., G. A., Baisie, M., Baraloto, C.,
453 Camargo, P. B., Barroso, J., Blanc, L., Bonal, D., Bongers, F., Boot, R., Brown, F., Burban, B., Camargo, J. L., Castro, W.,
454 Moscoso, V. C., Chave, J., Comiskey, J., Valverde, F. C., da Costa, A. L., Cardozo, N. D., Di Fiore, A., Dourdain, A., Erwin, T.,
455 Llampazo, G. F., Vieira, I. C. G., Herrera, R., Honorio Coronado, E., Huamantupa-Chuquimaco, I., Jimenez-Rojas, E., Killeen,
456 T., Laurance, S., Laurance, W., Levesley, A., Lewis, S. L., Ladvocat, K. L. L. M., Lopez-Gonzalez, G., Lovejoy, T., Meir, P.,
457 Mendoza, C., Morandi, P., Neill, D., Nogueira Lima, A. J., Vargas, P. N., de Oliveira, E. A., Camacho, N. P., Pardo, G.,
458 Peacock, J., Peña-Claros, M., Peñuela-Mora, M. C., Pickavance, G., Pipoly, J., Pitman, N., Prieto, A., Pugh, T. A. M., Quesada,
459 C., Ramirez-Angulo, H., de Almeida Reis, S. M., Rejou-Machain, M., Correa, Z. R., Bayona, L. R., Rudas, A., Salomão, R.,
460 Serrano, J., Espejo, J. S., Silva, N., Singh, J., Stahl, C., Stropp, J., Swamy, V., Talbot, J., ter Steege, H., et al.: Tree mode of
461 death and mortality risk factors across Amazon forests, *Nat Commun*, 11, 5515, <https://doi.org/10.1038/s41467-020-18996-3>,
462 2020.
- 463 Fisher, J. I., Hurtt, G. C., Thomas, R. Q., and Chambers, J. Q.: Clustered disturbances lead to bias in large-scale estimates based
464 on forest sample plots: Clustered disturbance and forest plot bias, 11, 554–563, <https://doi.org/10.1111/j.1461->
465 0248.2008.01169.x, 2008.
- 466 Fontes, C. G., Chambers, J. Q., and Higuchi, N.: Revealing the causes and temporal distribution of tree mortality in Central
467 Amazonia, *Forest Ecology and Management*, 424, 177–183, <https://doi.org/10.1016/j.foreco.2018.05.002>, 2018.
- 468 Garstang, M., White, S., Shugart, H. H., and Halverson, J.: Convective cloud downdrafts as the cause of large blowdowns in the
469 Amazon rainforest, *Meteorol. Atmos. Phys.*, 67, 199–212, <https://doi.org/10.1007/BF01277510>, 1998.



- 470 Hall, J., Muscarella, R., Quebbeman, A., Arellano, G., Thompson, J., Zimmerman, J. K., and Uriarte, M.: Hurricane-Induced
471 Rainfall is a Stronger Predictor of Tropical Forest Damage in Puerto Rico Than Maximum Wind Speeds, *Sci Rep*, 10, 4318,
472 <https://doi.org/10.1038/s41598-020-61164-2>, 2020.
- 473 Harms, K. E., Condit, R., Hubbell, S. P., and Foster, R. B.: Habitat associations of trees and shrubs in a 50-ha neotropical forest
474 plot: *Habitat associations of trees and shrubs*, 89, 947–959, <https://doi.org/10.1111/j.1365-2745.2001.00615.x>, 2001.
- 475 Holdridge, L. R.: Determination of World Plant Formations from Simple Climatic Data, 105, 367–368, 1947.
- 476 Hubbell, S. P., Foster, R. B., O'Brien, S. T., Harms, K. E., Condit, R., Wechsler, B., Wright, S. J., and Loo de Lao, S.: Light-Gap
477 Disturbances, Recruitment Limitation, and Tree Diversity in a Neotropical Forest, 283, 554–557,
478 <https://doi.org/10.1126/science.283.5401.554>, 1999.
- 479 IPCC: Summary for Policymakers, in: *Climate Change 2014, Mitigation of Climate Change. Contribution of Working Group III*
480 *to the Fifth Assessment Report of the Intergovernmental Panel on Climate Change*, Cambridge University Press, United
481 Kingdom and New York, NY, USA, 2014.
- 482 Jansen, P. A., Meer, P. J. V. der, and Bongers, F.: SPATIAL CONTAGIOUSNESS OF CANOPY DISTURBANCE IN
483 TROPICAL RAIN FOREST: AN INDIVIDUAL-TREE-BASED TEST, *Ecology*, 89, 3490–3502, [https://doi.org/10.1890/07-](https://doi.org/10.1890/07-1682.1)
484 [1682.1](https://doi.org/10.1890/07-1682.1), 2008.
- 485 Jaramillo, L., Poveda, G., and Mejía, J. F.: Mesoscale convective systems and other precipitation features over the tropical
486 Americas and surrounding seas as seen by TRMM: MESOSCALE CONVECTIVE SYSTEMS IN TROPICAL AMERICAS, *Int.*
487 *J. Climatol*, 37, 380–397, <https://doi.org/10.1002/joc.5009>, 2017.
- 488 Kellner, J. R. and Asner, G. P.: Convergent structural responses of tropical forests to diverse disturbance regimes, 12, 887–897,
489 <https://doi.org/10.1111/j.1461-0248.2009.01345.x>, 2009.
- 490 Leigh, E. G. Jr.: *Tropical forest ecology: a view from Barro Colorado Island*, Oxford University Press, Oxford, 1999.
- 491 Leitold, V., Morton, D. C., Longo, M., dos-Santos, M. N., Keller, M., and Scaranello, M.: El Niño drought increased canopy
492 turnover in Amazon forests, *New Phytol*, 219, 959–971, <https://doi.org/10.1111/nph.15110>, 2018.
- 493 Lobo, E. and Dalling, J. W.: Effects of topography, soil type and forest age on the frequency and size distribution of canopy gap
494 disturbances in a tropical forest, *Biogeosciences*, 10, 6769–6781, <https://doi.org/10.5194/bg-10-6769-2013>, 2013.
- 495 Lobo, E. and Dalling, J. W.: Spatial scale and sampling resolution affect measures of gap disturbance in a lowland tropical
496 forest: implications for understanding forest regeneration and carbon storage, *Proc. R. Soc. B.*, 281, 20133218,
497 <https://doi.org/10.1098/rspb.2013.3218>, 2014.
- 498 Manrubia, S. C. and Solé, R. V.: On Forest Spatial Dynamics with Gap Formation, *Journal of Theoretical Biology*, 187, 159–
499 164, <https://doi.org/10.1006/jtbi.1997.0409>, 1997.
- 500 Marra, D. M., Chambers, J. Q., Higuchi, N., and Trumbore, S. E.: Large-Scale Wind Disturbances Promote Tree Diversity in a
501 Central Amazon Forest, 9, 16, 2014.
- 502 Marvin, D. C. and Asner, G. P.: Branchfall dominates annual carbon flux across lowland Amazonian forests, *Environ. Res. Lett.*,
503 11, 094027, <https://doi.org/10.1088/1748-9326/11/9/094027>, 2016.
- 504 McDowell, N., Allen, C. D., Anderson-Teixeira, K., Brando, P., Brienen, R., Chambers, J., Christoffersen, B., Davies, S.,
505 Doughty, C., Duque, A., Espirito-Santo, F., Fisher, R., Fontes, C. G., Galbraith, D., Goodsman, D., Grossiord, C., Hartmann, H.,
506 Holm, J., Johnson, D. J., Kassim, Abd. R., Keller, M., Koven, C., Kueppers, L., Kumagai, T., Malhi, Y., McMahon, S. M.,
507 Mencuccini, M., Meir, P., Moorcroft, P., Muller-Landau, H. C., Phillips, O. L., Powell, T., Sierra, C. A., Sperry, J., Warren, J.,
508 Xu, C., and Xu, X.: Drivers and mechanisms of tree mortality in moist tropical forests, *New Phytol*, 219, 851–869,
509 <https://doi.org/10.1111/nph.15027>, 2018.
- 510 McMahon, S. M., Arellano, G., and Davies, S. J.: The importance and challenges of detecting changes in forest mortality rates,
511 *Ecosphere*, 10, e02615, <https://doi.org/10.1002/ecs2.2615>, 2019.



- 512 Muller-Landau, H. C., Condit, R. S., Harms, K. E., Marks, C. O., Thomas, S. C., Bunyavejchewin, S., Chuyong, G., Co, L.,
513 Davies, S., Foster, R., Gunatilleke, S., Gunatilleke, N., Hart, T., Hubbell, S. P., Itoh, A., Kassim, A. R., Kenfack, D., LaFrankie,
514 J. V., Lagunzad, D., Lee, H. S., Losos, E., Makana, J.-R., Ohkubo, T., Samper, C., Sukumar, R., Sun, I.-F., Nur Supardi, M. N.,
515 Tan, S., Thomas, D., Thompson, J., Valencia, R., Vallejo, M. I., Munoz, G. V., Yamakura, T., Zimmerman, J. K., Dattaraja, H.
516 S., Esufali, S., Hall, P., He, F., Hernandez, C., Kiratiprayoon, S., Suresh, H. S., Wills, C., and Ashton, P.: Comparing tropical
517 forest tree size distributions with the predictions of metabolic ecology and equilibrium models, *Ecol Letters*, 9, 589–602,
518 <https://doi.org/10.1111/j.1461-0248.2006.00915.x>, 2006a.
- 519 Muller-Landau, H. C., Condit, R. S., Chave, J., Thomas, S. C., Bohlman, S. A., Bunyavejchewin, S., Davies, S., Foster, R.,
520 Gunatilleke, S., Gunatilleke, N., Harms, K. E., Hart, T., Hubbell, S. P., Itoh, A., Kassim, A. R., LaFrankie, J. V., Lee, H. S.,
521 Losos, E., Makana, J.-R., Ohkubo, T., Sukumar, R., Sun, I.-F., Nur Supardi, M. N., Tan, S., Thompson, J., Valencia, R., Munoz,
522 G. V., Wills, C., Yamakura, T., Chuyong, G., Dattaraja, H. S., Esufali, S., Hall, P., Hernandez, C., Kenfack, D., Kiratiprayoon,
523 S., Suresh, H. S., Thomas, D., Vallejo, M. I., and Ashton, P.: Testing metabolic ecology theory for allometric scaling of tree size,
524 growth and mortality in tropical forests, *Ecol Letters*, 9, 575–588, <https://doi.org/10.1111/j.1461-0248.2006.00904.x>, 2006b.
- 525 Negrón-Juárez, R. I., Chambers, J. Q., Guimaraes, G., Zeng, H., Raupp, C. F. M., Marra, D. M., Ribeiro, G. H. P. M., Saatchi, S.
526 S., Nelson, B. W., and Higuchi, N.: Widespread Amazon forest tree mortality from a single cross-basin squall line event: WIND-
527 DRIVEN TREE MORTALITY IN AMAZONIA, *Geophys. Res. Lett.*, 37, n/a-n/a, <https://doi.org/10.1029/2010GL043733>,
528 2010.
- 529 Negrón-Juárez, R. I., Jenkins, H. S., Raupp, C. F. M., Riley, W. J., Kueppers, L. M., and Marra, D. M.: Windthrow Variability in
530 Central Amazonia, 17, 2017.
- 531 Negrón-Juárez, R. I., Holm, J. A., Marra, D. M., Rifai, S. W., Riley, W. J., Chambers, J. Q., Koven, C. D., Knox, R. G.,
532 McGroddy, M. E., Di Vittorio, A. V., Urquiza-Muñoz, J., Tello-Espinoza, R., Muñoz, W. A., Ribeiro, G. H. P. M., and Higuchi,
533 N.: Vulnerability of Amazon forests to storm-driven tree mortality, *Environ. Res. Lett.*, 13, 054021,
534 <https://doi.org/10.1088/1748-9326/aabe9f>, 2018.
- 535 Pan, Y., Birdsey, R. A., Phillips, O. L., and Jackson, R. B.: The Structure, Distribution, and Biomass of the World's Forests,
536 *Annu. Rev. Ecol. Evol. Syst.*, 44, 593–622, <https://doi.org/10.1146/annurev-ecolsys-110512-135914>, 2013.
- 537 Phillips, O. L., Lloyd, J., Malhi, Y., Monteagudo, A., Almeida, S., Davila, E. A., Amaral, I., Andelman, S., Andrade, A., Arroyo,
538 L., Aymard, G., Baker, T. R., and Bonal, D.: Drought–mortality relationships for tropical forests, 16, 2010.
- 539 Silva, C. A., Valbuena, R., Pinagé, E. R., Mohan, M., Almeida, D. R. A., North Broadbent, E., Jaafar, W. S. W. M., Papa, D.,
540 Cardil, A., and Klauberg, C.: ForestGapR: An r Package for forest gap analysis from canopy height models, *Methods Ecol Evol*,
541 10, 1347–1356, <https://doi.org/10.1111/2041-210X.13211>, 2019.
- 542 Silva, C. V. J., Aragão, L. E. O. C., Barlow, J., Espirito-Santo, F., Young, P. J., Anderson, L. O., Berenguer, E., Brasil, I., Foster
543 Brown, I., Castro, B., Farias, R., Ferreira, J., França, F., Graça, P. M. L. A., Kirsten, L., Lopes, A. P., Salimon, C., Scaranello, M.
544 A., Seixas, M., Souza, F. C., and Xaud, H. A. M.: Drought-induced Amazonian wildfires instigate a decadal-scale disruption of
545 forest carbon dynamics, *Phil. Trans. R. Soc. B*, 373, 20180043, <https://doi.org/10.1098/rstb.2018.0043>, 2018.
- 546 Solé, R. V. and Manrubia, S. C.: Are rainforests self-organized in a critical state?, *Journal of Theoretical Biology*, 173, 31–40,
547 <https://doi.org/10.1006/jtbi.1995.0040>, 1995.
- 548 Windsor, D. M.: Climate and moisture variability in a tropical forest: long-term records from Barro Colorado Island, Panamá,
549 *Smithsonian Contributions to the Earth Sciences*, 29, 1–45, <https://doi.org/10.5479/si.00810274.29.1>, 1990.
- 550 Yanoviak, S. P., Gora, E. M., Burchfield, J. M., Bitzer, P. M., and Detto, M.: Quantification and identification of lightning
551 damage in tropical forests, *Ecol Evol*, 7, 5111–5122, <https://doi.org/10.1002/ece3.3095>, 2017.
- 552 Zahawi, R. A., Dandois, J. P., Holl, K. D., Nadwodny, D., Reid, J. L., and Ellis, E. C.: Using lightweight unmanned aerial
553 vehicles to monitor tropical forest recovery, *Biological Conservation*, 186, 287–295,
554 <https://doi.org/10.1016/j.biocon.2015.03.031>, 2015.

555